Arrangement of Substrates at the Active Site of an Aminoglycoside Antibiotic 3′-Phosphotransferase As Determined by NMR

James R. Cox,[†] Geoffrey A. McKay,[‡] Gerard D. Wright,[‡] and Engin H. Serpersu*[,†]

Contribution from the Departments of Biochemistry, The University of Tennessee, Knoxville, Tennessee 37996-0840, and McMaster University, Hamilton, Ontario, Canada L8N 3Z5

Received August 30, 1995[⊗]

Abstract: The arrangements of the antibiotics amikacin and butirosin A at the active site of an aminoglycoside antibiotic 3′-phosphotransferase (APH(3′)-IIIa), which mediates resistance to a broad spectrum of aminoglycoside antibiotics, were determined. APH(3′)-IIIa phosphorylates a wide range of aminoglycoside antibiotics in an ATP-dependent manner. β,γ-Bidentate CrATP, a stable exchange-inert metal−nucleotide analog, was used as a paramagnetic probe to determine the arrangement of amikacin and butirosin A in the respective enzyme·CrATP·-antibiotic complexes. The paramagnetic effects of Cr^{3+} on the longitudinal relaxation rates ($1/T_{1p}$) of the ^1H nuclei of amikacin and butirosin A were examined to determine the distances between enzyme-bound CrATP and various protons of these aminoglycoside antibiotics in the ternary APH(3′)-IIIa·CrATP·antibiotic complexes. From these distances, models were constructed that represent possible enzyme-bound arrangements and conformations for these aminoglycosides. These models show that amikacin and butirosin A adopt different arrangements at the active site of APH(3′)-IIIa. The results for butirosin A suggest that the 2,6-diamino-2,6-dideoxy-D-glucose and D-xylose rings are in a stacking arrangement which is consistent with its solution structure. This is the first paper to describe the arrangement and conformation of aminoglycoside antibiotics bound to a modifying enzyme and is an important step in the design of novel antibiotics and/or enzyme inhibitors.

Introduction

Bacterial resistance to antibiotics is currently at a crisis level and has been declared a public health emergency.[1,2] The once seemingly formidable array of effective antibiotics is declining, thus making previously treatable infections life-threatening.[3] One of the most alarming examples of antibiotic resistance is that in Gram-positive cocci, which are responsible for a large fraction of hospital-acquired infections.[4,5] Enterococcal and staphylococcal infections are typically treated through the administration of aminoglycoside antibiotics, which area class of aminocyclitol antibiotics that bind to the bacterial 30S ribosomal subunit. They interfere with normal protein biosynthesis which ultimately leads to cell death.[6] Bacteria have responded to the evolutionary pressure brought about by the use of these drugs by expressing an array of enzymes which covalently modify aminoglycosides, thereby rendering them inoffensive.[7,8] The expression of several distinct classes of aminoglycoside 3′-phosphotransferase (APH(3′)) enzymes have been reported.[9] These enzymes, found in many pathogenic bacteria, modify the aminoglycosides at the 3′-position and have essentially eliminated the clinical utility of formerly useful aminoglycosides possessing a 3′-OH group such as kanamycin.

Recently, the overexpression and characterization of an enterococcal aminoglycoside 3′-phosphotransferase, APH(3′)-IIIa, has been reported.[10] This enzyme phosphorylates a broad spectrum of aminoglycoside antibiotics at the 3′-OH group such as kanamycin, amikacin, butirosin A, neomycin B, paramomycin, and ribostamycin in an ATP-dependent manner. Lividomycin, which is a 3′-deoxyaminoglycoside, is also a substrate for the enzyme, providing evidence for 5″-phosphotransferase activity. The elucidation of the conformation and arrangement of aminoglycosides at the active site of APH(3′)-IIIa will be an important step in understanding the broad substrate specificity of this enzyme. Also, knowledge of how aminoglycosides occupy the active site of APH(3′)-IIIa will bring insight into the molecular mechanism in which aminoglycosides are inactivated. This information will be valuable in an attempt to design novel antibiotics and/or enzyme inhibitors that could be used to recapture the effectiveness of aminoglycoside antibiotics.

The knowledge of the molecular basis of enzymatic catalysis is dependent upon the collection of dependable structural information on enzyme-bound substrate complexes. Measurement of the paramagnetic relaxation rates ($1/T_{1p}$) of substrate magnetic nuclei (protons), in the presence of a paramagnetic probe, allows for the calculation of distances from the ^1H nuclei of an enzyme-bound molecule in solution to a paramagnetic center.[11,12] Information about the conformation and arrangement of enzyme-bound substrates can be derived from the paramagnetic distances.

* To whom correspondence should be addressed. Phone: (423) 974-2668. FAX: (423) 974-6306. E-mail: SERPERSU@utkvx.utk.edu.
[†] The University of Tennessee.
[‡] McMaster University.
[⊗] Abstract published in *Advance ACS Abstracts,* February 1, 1996.
(1) Kunin, C. M. *Ann. Intern. Med.* **1993**, *118*, 557.
(2) Berkelman, R. L.; Hughes, J. M. *Ann. Intern. Med.* **1993**, *119*, 426.
(3) Hyde, B. *ASM News* **1994**, *60*, 243.
(4) Moellering, R. C. *J. Antimicrob. Chemother.* **1991**, *28*, 1.
(5) Tomasz, A. *N. Engl. J. Med.* **1994**, *330*, 1247.
(6) Davies, B. D. *Microbiol. Rev.* **1987**, *51*, 341.
(7) Davies, J. *Science* **1994**, *264*, 375.
(8) Umezawa, H.; Kondo, S. In *Aminoglycoside Antibiotics*; Umezawa, H., Hooper, I. R., Eds.; Springer-Verlag: Berlin, 1982; p 267.
(9) Shaw, K. J.; Rather, P. N.; Hare, R. S.; Miller, G. H. *Microbiol. Rev.* **1993**, *57*, 138.
(10) McKay, G. A.; Thompson, P. R.; Wright, G. D. *Biochemistry* **1994**, *33*, 6936.
(11) Mildvan, A. S.; Gupta, R. K. *Methods Enzymol.* **1978**, *44G*, 322.
(12) Mildvan, A. S.; Cohn, M. *Adv. Enzymol.* **1970**, *33*, 1.

0002-7863/96/1518-1295$12.00/0

β,γ-Bidentate $Cr(H_2O)_4ATP$ (CrATP) is a stable exchange-inert metal−ATP analog, which has been successfully used as a paramagnetic probe for intersubstrate distance measurements.[13−16] In this study, CrATP was used to explore the conformation and arrangement of amikacin and butirosin A at the active site of APH(3′)-IIIa in order to better understand the molecular details of the inactivation chemistry that renders the aminoglycosides inoffensive.

Experimental Section

Materials. The overexpression and purification of APH(3′)-IIIa has been described previously.[10] β,γ-Bidentate CrATP was prepared immediately before use as described[17] and diluted with ^2H_2O for ^1H NMR experiments. ^2H_2O (99.9 and 99.96 atom %) was purchased from Isotec, Inc., and Wilmad, respectively. Deuterium chloride and sodium deuteroxide (both 99.9 atom %) were from MSD Isotopes. Amikacin, butirosin A (sulfate salt), ATP, NADPH, the dicyclohexylammonium salt of phosphoenolpyruvate (PEP) and 2-morpholinoethanesulfonic acid (MES) were obtained from Sigma Chemical Co. Pyruvate kinase (PK) and lactate dehydrogenase (LDH) were obtained from Boehringer Mannheim. All other chemicals used were of the highest grade commercially available.

Magnetic Resonance Studies. The paramagnetic effect of CrATP on the relaxation rates of the protons of the aminoglycoside antibiotics amikacin and butirosin A bound in ternary (CrATP·APH(3′)-IIIa·-antibiotic) and binary (CrATP·antibiotic) complexes were determined at 400 MHz (Bruker AMX-400 wide-bore spectrometer). The inversion recovery method was used with 500 μL samples in ^2H_2O and 14 variable delays ranging from 20 ms to 7 s. Despite the multiplicity of resonances, the inversion recovery plots were not multiphasic within the time range used to determine T_1.

APH(3′)-IIIa was first dialyzed against 2 mM deuterated Tris ([^{2}H]-Tris) buffer (pH 6.8) in order to avoid the interference of Tris protons. The enzyme was then exchanged into ^2H_2O by three cycles of lyophilization and redissolving in ^2H_2O. The aminoglycosides were dissolved directly into ^2H_2O, underwent two cycles of lyophilization, and were redissolved in ^2H_2O. Samples contained 0.20−0.30 mM APH(3′)-IIIa, 7 mM amikacin or 6 mM butirosin A, 50 mM NaCl, and 20 mM [^{2}H]Tris (pH 6.8). The solution was then titrated with CrATP, and the increases in the longitudinal relaxation rates ($1/T_1$) of various protons of the antibiotics were measured. The data were analyzed by plotting the relaxation rates against the concentration of CrATP bound in the ternary CrATP·APH(3′)-IIIa·antibiotic complexes. The slopes of these curves were then corrected by subtracting the contribution of the paramagnetic effects of CrATP in the binary CrATP·antibiotic complex that was based on the known distribution of CrATP among the binary and ternary complexes, as calculated from the respective dissociation constants. The corrected slopes obtained in this fashion, when multiplied by the total antibiotic concentration, yielded the normalized relaxation rates ($1/fT_{1p}$), where f is defined as [bound CrATP]/[antibiotic]. The temperature dependence of $1/T_1$ of the protons of amikacin and butirosin A in the ternary complex was examined at 12, 23, and 32 °C for amikacin and 22, 32, and 42 °C for butirosin A. Sample composition was as described above for the analysis of the paramagnetic effect of CrATP on the protons of amikacin and butirosin A in the ternary complex.

Longitudinal relaxation rates of water protons were determined with a Seimco pulsed NMR spectrometer at 24.3 MHz as previously described[18,19] using the $180°-\tau-90°$ pulse sequence of Carr and Purcell[20] and a delay of $5T_1$ to allow for complete relaxation. The paramagnetic contribution (T_1 values) to relaxation rates ($1/T_{1p}$) and evaluation of enhancements of the paramagnetic effects of CrATP were determined as described previously.[18,19,21] The observed enhancement of the relaxation rate is defined as $\epsilon = (1/T_{1p})^*/(1/T_{1p})$, where the asterisk denotes the presence of the macromolecular species. The enhancement values for the binary CrATP·amikacin and CrATP·-butirosin complexes (ϵ_a) and APH(3′)-IIIa·CrATP complex (ϵ_b) were determined and were used to calculate the fraction of bound CrATP. To determine the dissociation constant of the antibiotics in the ternary APH(3′)-IIIa·CrATP·antibiotic complexes, solutions of MES (50 mM, pH 6.5), APH(3′)-IIIa (200 μM), and CrATP (100 and 200 μM) were titrated with the antibiotics (0−3.5 mM) while monitoring the $1/T_1$ of water protons. The dissociation constants (K_3) were determined by computer fitting as described previously.[18,22]

The correlation time for the dipolar electron nucleus interaction in the ternary APH(3′)-IIIa·CrATP·antibiotic complex was determined by studying the frequency dependence of $1/T_{1p}$ of water protons at 90 MHz on a FX 90Q Jeol spectrometer, 250 MHz on a Bruker AC250 spectrometer, and 400 MHz on a Bruker AMX-400 wide-bore spectrometer by the inversion recovery method as described previously.[18,19] Evaluation of τ_c from the frequency-dependent $1/T_{1p}$ values was done by computer fitting as described earlier.[11,18,22] Samples contained 20 mM Tris (pH 6.8), 0.6 mM APH(3′)-IIIa, 8 μM CrATP, and 5 mM antibiotic. Corrections were made to account for the paramagnetic effect of free CrATP on the observed relaxation rates.

Samples for the transferred nuclear Overhauser effect spectroscopy (NOESY) experiments were prepared as described above except that they contained 200 μM APH(3′)-IIIa, 5 mM antibiotic, 5 mM ATP, and 5 mM $CaCl_2$. The NOESY spectra were collected in the phase-sensitive mode with the transmitter offset placed on the H^2HO resonance, which was irradiated during the relaxation delay of 1.8 s to suppress the H_2O signal. A total of 256 FIDs of 2k were collected. Mixing times of 40, 80, 120, and 160 ms were employed, and the data were zero-filled to 1k points in t_1 and were multiplied by a shifted $\sin^2$ window function before Fourier transformation. Data and NOE analyses were performed in a FELIX (Version 2.30, Biosym Technologies) NMR processing program operating on a Silicon Graphics Indigo^2 workstation.

Kinetic and Inactivation Studies. The inhibition of APH(3′)-IIIa activity by CrATP was measured by following the oxidation of NADH at 340 nm in a coupled enzyme assay system. This was accomplished by coupling the release of ADP (from kanamycin phosphorylation) to a pyruvate kinase/lactate dehydrogenase reaction system. The reaction mixture contained 100 mM KCl, 50 mM MES (pH 6.5), 2 mM PEP (cyclohexylammonium salt), 0.2 mM NADH, 0.25 mM kanamycin A, 36 μL of a pyruvate kinase (200 U/mg) suspension, and 20 μL of a lactate dehydrogenase (550 U/mg) suspension. All reaction mixtures contained 30 μg/mL APH(3′)-IIIa, and ATP concentrations ranged from 0.03 to 0.50 mM. CrATP concentrations used were 0, 0.05, 0.20, and 0.40 mM, and the concentration of $MgCl_2$ in each assay was 1 mM greater than the ATP concentration. Rate measurements were carried out by monitoring the loss of absorbance at 340 nm on a Beckman DU-70 spectrophotometer at 25 °C.

The inactivation of APH(3′)-IIIa by CrATP was performed at a concentration of 1.5 μg/μL enzyme in a total volume of 300 μL at 37 °C. The incubation reaction mixture also contained 0.5 mM kanamycin A in 50 mM MES (pH 6.5) and various CrATP concentrations such as 0.075, 0.100, 0.150, 0.250, 0.500, and 3.00 mM. At different time points between 0 and 235 min, 5 μL aliquots were removed from the incubation mixture and the remaining enzyme activity was measured. Enzyme activity was measured as described above except that CrATP was not present in any of the reaction mixtures and the concentrations of ATP and $MgCl_2$ in the reaction mixture were 10 and 20 mM, respectively. All of the inactivation data were fitted to a first-order decay by P Fit software (Biosoft) using the equation $y = Ae^{-kt} + C$ (constant).

(13) Gupta, R. K.; Fung, C. H.; Mildvan, A. S. *J. Biol. Chem.* **1976**, *251*, 2421.
(14) Fry, D. C.; Kuby, S. A.; Mildvan, A. S. *Biochemistry* **1985**, *24*, 4680.
(15) Wolkers, W. F.; Gregory, J. D.; Churchich, J. E.; Serpersu, E. H. *J. Biol. Chem.* **1991**, *31*, 20761.
(16) Gregory, J. D.; Serpersu, E. H. *J. Biol. Chem.* **1993**, *268*, 3880.
(17) Dunaway-Mariano, D.; Cleland, W. W. *Biochemistry* **1980**, *19*, 1496.
(18) Serpersu, E. H.; Shortle, D.; Mildvan, A. S. *Biochemistry* **1987**, *26*, 1289.
(19) Mildvan, A. S.; Engle, J. L. *Methods Enzymol.* **1972**, *26C*, 654.
(20) Carr, H. Y.; Purcell, E. M. *Physiol. Rev.* **1954**, *94*, 630.
(21) Serpersu, E. H.; McCracken, J.; Peisach, J.; Mildvan, A. S. *Biochemistry* **1988**, *27*, 8034.
(22) Serpersu, E. H.; Shortle, D.; Mildvan, A. S. *Biochemistry* **1986**, *25*, 68.

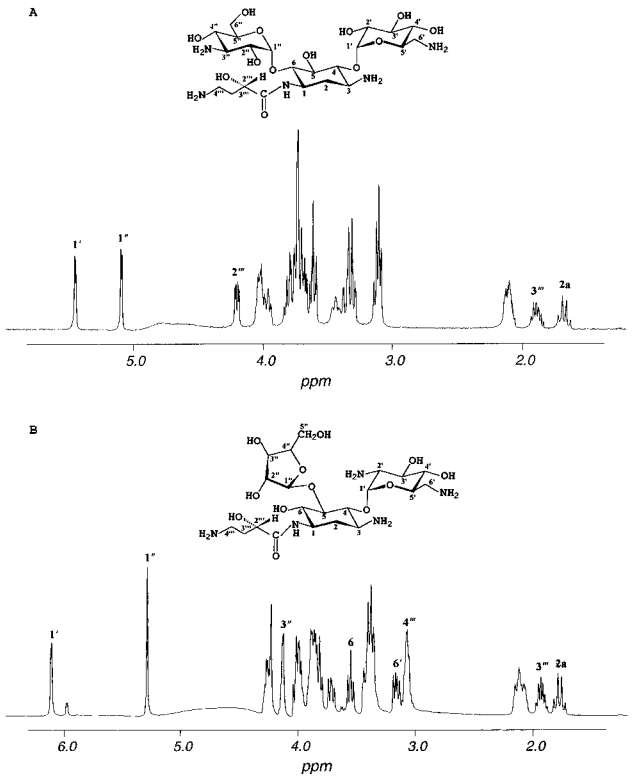

Figure 1. Structures and 1D ^{1}H NMR spectra of amikacin (A) and butirosin A (B) with the resonances used in this study marked above with the appropriate proton. The spectra were processed and the solvent peak was removed with FELIX (Biosym Technologies) software. The ^{1}H assignments of butirosin A[23] and amikacin[24] have been previously reported.

Results and Discussion

Aminoglycoside Structure and NMR. The structures of amikacin and butirosin A and the 1D ^{1}H NMR spectra of these antibiotics appear in Figure 1. The primed ring is 6-amino-6-deoxy-D-glucose in amikacin and 2,6-diamino-2,6-dideoxy-D-glucose in butirosin A. The double primed ring is 3-amino-3-deoxy-D-glucose in amikacin and D-xylose in butirosin A. The unprimed ring in amikacin and butirosin A is 2-deoxystreptamine modified at N-1 with a (*S*)-4-amino-2-hydroxybutyryl group (AHB), which is denoted with a triple prime.

The ^{1}H assignments of the antibiotics were necessary in these studies to determine the arrangement of bound substrates. The complete ^{1}H assignments of butirosin A were reported from this laboratory,[23] and the ^{1}H resonances of amikacin have been previously assigned.[24] The overlap in the ^{1}H NMR spectra dictates which protons can be used in the distance determinations, and the 1D ^{1}H NMR spectra are provided here to show which protons could be used in Cr^{3+}-to-^{1}H distance calculations. It was quite fortuitous that several protons were isolated in both spectra which allowed Cr^{3+}-to-^{1}H distances to be measured in each ring and the AHB chain of the antibiotics.

Kinetic Studies. To use CrATP as a paramagnetic probe with APH(3′)-IIIa, it was first necessary to demonstrate that CrATP binds to the active site of the enzyme. Kinetic analysis of the inhibition of APH(3′)-IIIa by CrATP showed that CrATP is a linear competitive inhibitor with respect to MgATP and yielded a K_{is} for CrATP of 124 ± 16 μM. Incubation of APH(3′)-IIIa with various concentrations of CrATP showed a time-dependent pseudo-first-order loss of enzyme activity. The rate of inactivation was dependent on the concentration of CrATP and showed saturation behavior (Figure 2). This type of kinetic behavior is consistent with the formation of a long-lived APH(3′)-IIIa·CrATP complex. Since Cr^{3+} exchanges its ligands very slowly, it is likely that this complex may be formed by donation of a ligand from the enzyme to the coordination sphere of Cr^{3+}. The pseudo-first-order rate constants (k_{obs}) for each concentration of CrATP were determined and plotted in double reciprocal form ($1/k_{obs}$ vs 1/[CrATP]). This is a linear plot which yielded an inactivation rate of 0.024 ± 0.005 min^{-1} and a K_{is} for CrATP of 88 ± 26 μM (eq 1). The results from the kinetic studies suggest that CrATP does indeed bind to the active site of APH(3′)-IIIa and can be used as a paramagnetic probe.

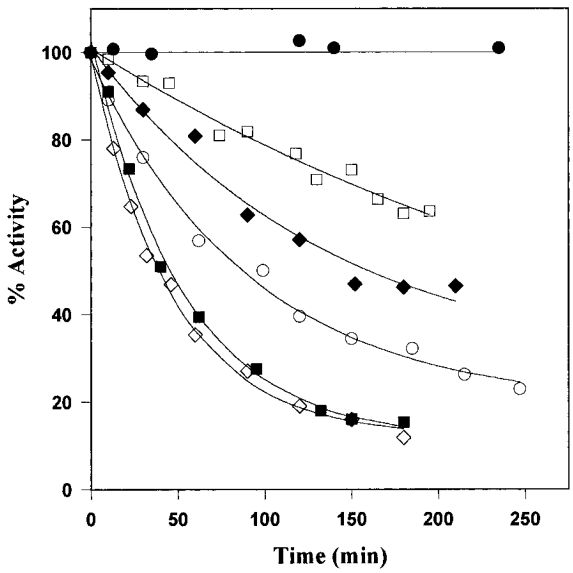

Figure 2. Inactivation of APH(3′)-IIIa by CrATP. The enzyme was incubated at 37 °C in 50 mM MES (pH 6.5), 0.5 mM kanamycin A, and CrATP. CrATP concentrations used were (●) 0 mM, (□) 0.025 mM, (◆) 0.040 mM, (○) 0.075 mM, (■) 0.250 mM, and (◇) 3.00 mM.

$$E + I \rightleftarrows EI \rightleftarrows EI^* \qquad (1)$$

Binding Studies. The binding of CrATP to the enzyme was studied by pulsed NMR spectroscopy at 24.3 MHz.[18,19,22] APH(3′)-IIIa·CrATP complex formation was indicated by an increase in the enhancement (ϵ^*) of the paramagnetic effect of CrATP on the longitudinal relaxation rates ($1/T_{1p}$) of water protons when the enzyme was titrated with CrATP. A double reciprocal plot of the data ($1/\epsilon^*$ vs 1/[APH(3′)-IIIa]) yielded a straight line which describes the enhancement of $1/T_{1p}$ of water protons (ϵ_b) resulting from the binding of CrATP to the enzyme. The value of ϵ_b in this case was 1.88, which is similar to the values found with other CrATP·enzyme complexes.[13,16] The relaxation data were used to determine the stoichiometry of binding and the dissociation constant for the CrATP·enzyme complex through a Scatchard analysis. A K_D of 238 ± 32 μM with a 1:1 binding stoichiometry was determined for the CrATP·APH(3′)-IIIa complex from a Scatchard plot (not shown). For subsequent studies to be interpretable, it is important that only one paramagnetic probe is bound per active site of the enzyme. The approximate (3-fold) agreement between K_{is} of CrATP, determined by reversible, irreversible, and direct binding studies, is reasonable.

Binary CrATP·antibiotic complexes were also studied in a manner similar to that described above for the CrATP·APH(3′)-IIIa complex using amikacin and butirosin A. Dissociation constants of 11.8 and 14.1 mM and enhancement values (ϵ_a) of

(23) Cox, J. R.; Serpersu, E. H. *Carbohydr. Res.* **1995**, *271*, 55.
(24) Anderson, N. H.; Eaton, H. L.; Nguyen, E. T.; Hartzell, C.; Nelson, R. J.; Priest, J. H. *Biochemistry* **1988**, *27*, 2782.

Table 1. Dissociation constants (mM) and Enhancement Values (ϵ_T) of the APH(3′)-IIIa·CrATP·Antibiotic Complexes

constant[a–c]	amikacin	butirosin A	constant[a–c]	amikacin	butirosin A
K_D	0.238	0.238	K_3	0.263	0.025
K_1	11.8	14.0	K_2	0.005	0.0004
K_S	0.591	0.056	ϵ_T	2.78	2.23
K_A'	0.106	0.106			

[a] Binary dissociation constants are $K_D = [CrATP]_f[APH(3')\text{-}IIIa]_f/[APH(3')\text{-}IIIa\cdot CrATP]$, $K_S = [antibiotic]_f[APH(3')\text{-}IIIa]_f/[APH(3')\text{-}IIIa\cdot antibiotic]$, and $K_1 = [CrATP]_f[antibiotic]_f/[CrATP\cdot antibiotic]$. [b] Ternary dissociation constants are $K_A' = [CrATP]_f[APH(3')\text{-}IIIa\cdot antibiotic]/[APH(3')\text{-}IIIa\cdot CrATP\cdot antibiotic]$, $K_2 = [APH(3')\text{-}IIIa]_f[CrATP\cdot antibiotic]/[APH(3')\text{-}IIIa\cdot CrATP\cdot antibiotic]$, and $K_3 = [antibiotic]_f[APH(3')\text{-}IIIa\cdot CrATP]/[APH(3')\text{-}IIIa\cdot CrATP\cdot antibiotic]$. [c] Note that $K_1K_2 = K_3K_D = K_A'K_S$.

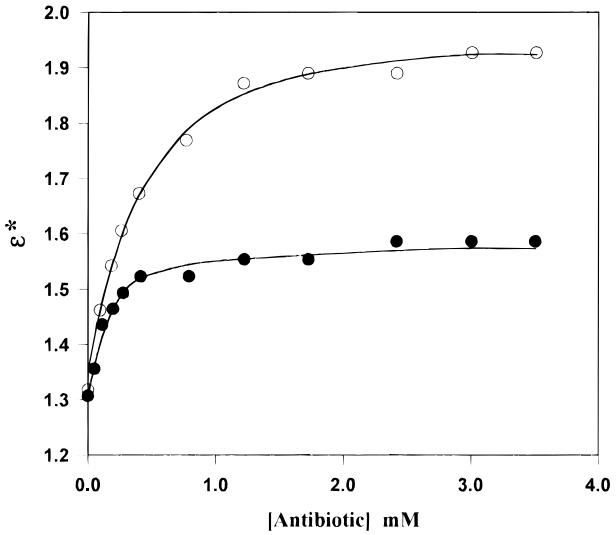

Figure 3. Changes in the observed enhancement (ϵ*) of the paramagnetic effects of CrATP on $1/T_1$ of water protons as amikacin (○) and butirosin A (●) form their respective ternary APH(3′)-IIIa·CrATP·-antibiotic complexes. The antibiotics (0−3.5 mM) were titrated into a solution that initially contained 50 mM MES (pH 6.5), 100 μM APH-(3′)-IIIa, and 100 μM CrATP.

1.43 and 1.59 were determined for amikacin and butirosin A, respectively.

The thermodynamic properties of a ternary system of enzyme, CrATP, and antibiotic is described by six equilibrium constants which have been described previously (Table 1).[18,22,25] To determine K_3, the dissociation constant of the antibiotic from the ternary APH(3′)-IIIa·CrATP·antibiotic complex, solutions of APH(3′)-IIIa and CrATP were titrated with antibiotics and the enhancement of $1/T_{1p}$ of water protons was measured. Representative titrations, with amikacin and butirosin A, are shown in Figure 3 with the computer-fitted curves.[18,21] K_3 values of 263 and 24.9 μM were determined for amikacin and butirosin A, respectively. All of the relevant dissociation constants determined in this study are given in Table 1. As shown in Figure 3, conversion of the binary APH(3′)-IIIa·-CrATP complex to the ternary APH(3′)-IIIa·CrATP·antibiotic complex increases the observed enhancement of $1/T_{1p}$ of water protons by the bound CrATP ($\epsilon_T > \epsilon_b$). This suggests that the immediate environment of Cr^{3+} is altered as the antibiotic binds to APH(3′)-IIIa to form the ternary complex. The observed differences in ϵ_T for amikacin and butirosin A reflect structural differences in the coordination sphere of Cr^{3+} in the respective ternary complexes. Also, K_3 for amikacin is higher than K_3 for butirosin A by an order of magnitude. These findings are in agreement with the kinetic studies which yielded K_m values of 245 and 34 μM for amikacin and butirosin A, respectively.[10] The observed differences between the antibiotics may reflect the orientation of substituents of the 2-deoxystreptamine ring since amikacin is 4,6-disubstituted and butirosin A is 4,5-disubstituted. However, examination of the kinetic data[10] suggests that K_m values for other antibiotics with 4,6- or 4,5-disubstitutions are different only by a factor of 2 or 3. Amikacin and butirosin A are substituted with an AHB chain at N-1 of the 2-deoxystreptamine ring. As suggested by McKay *et al.*,[10] AHB substitution may interfere with some antibiotic−enzyme interactions. Amikacin and butirosin A were used in this study because they were found to be in fast exchange from enzyme−substrate complexes, a condition necessary for the NMR experiments described below.

Comparison of K_S, the dissociation constant for the binary APH(3′)-IIIa·antibiotic complexes, and K_3 values for amikacin and butirosin A reveals that CrATP increases the affinity of both antibiotics to the enzyme by a factor of 2 (Table 1). This suggests that when the nucleotide is bound to the enzyme, the geometry of the active site is altered to create more favorable interactions between the side chains of APH(3′)-IIIa and the antibiotics. These data are also consistent with the kinetic data showing the mutual lowering of K_m values by ATP and antibiotic substrates.

Paramagnetic Effects of CrATP on the Protons of Amikacin and Butirosin A. The paramagnetic effect of CrATP on the relaxation rates of antibiotic protons was measured to determine Cr^{3+}-to-^{1}H distances in the ternary APH(3′)-IIIa·-CrATP·antibiotic complexes. Titration of CrATP into samples containing butirosin or amikacin and APH(3′)-IIIa resulted in an increase in the $1/T_1$ values of the antibiotic protons. Figure 4 shows the observed paramagnetic effects of enzyme-bound CrATP on the longitudinal relaxation rates ($1/T_1$) of various protons of amikacin and butirosin A. To correct for the effects of free CrATP and the binary CrATP·antibiotic complex, similar titrations were carried out in the absence of APH(3′)-IIIa. Comparison of the paramagnetic effects of CrATP on the $1/T_1$ values of the antibiotic protons in the binary CrATP·antibiotic and ternary enzyme·CrATP·antibiotic complexes shows that the presence of APH(3′)-IIIa causes an enhancement of the paramagnetic effects. The corrected and normalized paramagnetic effects ($1/fT_{1p}$) were then used to determine Cr^{3+}-to-^{1}H distances after justifying that they contain distance information as described in the next section.[16,21]

Determination of Correlation Time and Evaluation of the Temperature Dependence of $1/T_1$ of the Protons of Amikacin and Butirosin A. The temperature dependence of $1/T_1$ of the protons of amikacin and butirosin A were examined to establish that these antibiotics are in fast exchange from the APH(3′)-IIIa·CrATP·antibiotic ternary complexes. This is a necessary condition in the evaluation of distances in the paramagnetic ternary complex. Increasing relaxation rates with increasing temperature are indicative of exchange limitation since exchange rates ($1/\tau_M$) increase at higher temperatures. Fast exchange is indicated by a decrease in the relaxation rate with increasing temperature, which was observed for various protons of butirosin A and amikacin. Therefore, the observed relaxation values can be used for distance calculations. Determination of metal-to-nucleus distances, from the measurement of relaxation rates, requires a measurement of τ_c, the correlation time for the dipolar Cr^{3+}−nucleus interaction. The value of τ_c was evaluated by measuring the $1/T_{1p}$ of solvent water protons of samples at three frequencies. The paramagnetic contributions to $1/T_{1p}$ were observed at 90, 250, and 400 MHz for the ternary complexes

(25) Mildvan, A. S.; Cohn, M. *J. Biol. Chem.* **1966**, *241*, 1178.

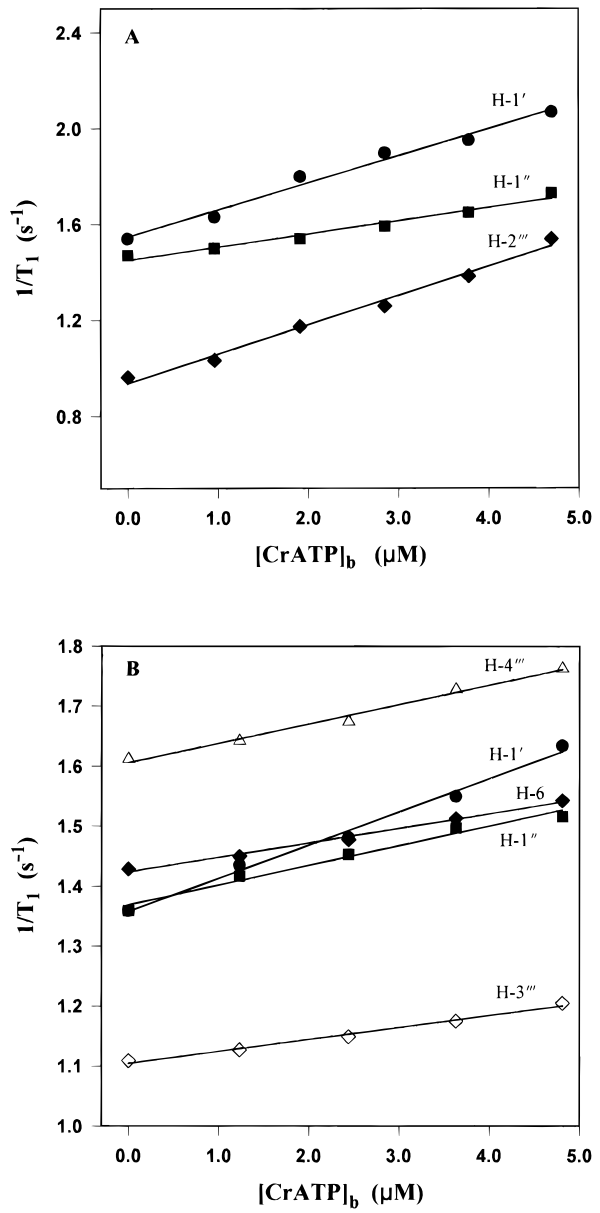

Figure 4. Paramagnetic effect of bound CrATP on representative protons of amikacin (A) and butirosin A (B). CrATP was titrated in samples that initially contained 0.20−0.30 mM APH(3′)-IIIa, 7 mM amikacin or 6 mM butirosin A, and 50 mM NaCl. The above data had to be corrected to account for the paramagnetic effects of CrATP in the CrATP·antibiotic complexes to obtain corrected $1/fT_{1p}$ values. The protons indicated for amikacin (A) are (●) H-1′, (■) H-1″, and (◆) H-2‴. The protons indicated for butirosin A (B) are (●) H-1′, (■) H-1″, (◆) H-6, (◇) H3‴, and (Δ) H4‴.

of the two antibiotics. The measured relaxation rates were corrected to account for the contribution of free CrATP to the observed relaxation rates. The τ_c values for the ternary APH(3′)-IIIa·CrATP·antibiotic complexes are presented in Table 2 and were determined by using a least-squares fitting program with a 5% error. These values are similar to those observed earlier for enzyme-bound CrATP complexes.[13−16] In addition, the frequency dependence of relaxation rates is also consistent with fast exchange conditions since exchange rates are not dependent on frequency.

Determination of Cr^{3+}-to-^1H Distances in the Ternary Complexes and the Arrangement of Substrates at the Active Site of APH(3′)-IIIa. The metal-nucleus distances can be determined from the normalized relaxation rates ($1/fT_{1p}$) of the bound antibiotic protons with the following equation:[11]

Table 2. Correlation Time and Other Parameters That Describe the Interaction of CrATP and APH(3′)-IIIa in the Ternary APH(3′)-IIIa·CrATP·Antibiotic Complexes

antibiotic	τ_c[a] (s)	$f(\tau_c)$ (s)	τ_v	B (s^{-2})
amikacin	1.09×10^{-9}	3.85×10^{-10}	1.06×10^{-12}	1.58×10^{21}
butirosin A	0.91×10^{-9}	4.39×10^{-10}	0.71×10^{-12}	1.50×10^{21}

[a] Determined from the frequency dependence of the longitudinal relaxation rates ($1/fT_{1p}$) of water protons at 90, 250, and 400 MHz and analyzed according to the equations[11] $1/\tau_c \sim 1/\tau_s = B(\tau_v/(1 + \omega_s^2\tau_v^2) + 4\tau_v/(1 + 4\omega_s^2\tau_v^2))$ and $f(\tau_c) = 3\tau_c/(1 + \omega_I^2\tau_c^2) + 7\tau_c/(1 + \omega_s^2\tau_c)$ were τ_c is the dipolar correlation time, τ_s is the longitudinal electron spin relaxation time, B is the zero-field splitting parameter, τ_v is a time constant for ligand motion that modulates B, and ω_s and ω_I are the electron and nuclear presession frequencies, respectively. The correlation times shown above are from the best fitted curve to the $1/fT_{1p}$ values determined at each frequency. The values for B and τ_v were obtained from the data analysis for each antibiotic.

Table 3. Corrected Relaxation Rates and Cr^{3+}−Proton Distances in the APH(3′)-IIIa·CrATP·Antibiotic Complexes

	amikacin		butirosin A	
proton	$1/fT_{1p}$[a] (s^{-1})	distance[b] (Å)	$1/fT_{1p}$ (s^{-1})	distance (Å)
2a	194	7.90 ± 0.58	*c*	>11
6			25	11.4 ± 0.84
1′	730	6.34 ± 0.47	175	8.22 ± 0.61
6′			225	7.88 ± 0.64
1″	223	7.72 ± 0.57	100	9.02 ± 0.67
3″			100	9.02 ± 0.67
2‴	421	6.95 ± 0.51		
3‴	447	6.88 ± 0.51	124	8.70 ± 0.64
4‴			112	8.85 ± 0.65

[a] The normalized reaction rates ($1/fT_{1p}$) were determined from the slope of the lines shown in Figure 4. [b] The errors shown in the absolute distances include 10%, 8%, and 30% due to the experimental errors in the measurements of $1/fT_{1p}$, τ_c, and the dissociation constant of CrATP from the ternary complex, respectively. [c] A correction of the relaxation rate due to the binary contribution was not possible due to the high relaxation rate of this proton in the binary CrATP·antibiotic complex.

$$r = C[(qfT_{1p})f(\tau_c)]^{1/6}$$

where r is the internucleus distance, C is a constant equal to 705 Å/$s^{1/3}$ for interactions between Cr^{3+} and protons,[26] q is the stoichiometry, and $f(\tau_c)$ is the correlation function which is described in Table 2. The normalized paramagnetic relaxation rates and distance measurements are given in Table 3. From these distances, models were built that represent possible arrangements for amikacin and butirosin A at the active site of APH(3′)-IIIa. The models presented in Figures 5 and 6 were constructed and analyzed in Insight II (Biosym Technologies) software on a Silicon Graphics Indigo^2 workstation and contain no van der Waals overlap between the atoms.

Amikacin is 4,6-disubstituted at the 2-deoxystreptamine ring and is regiospecifically phosphorylated at the 3′-OH by APH(3′)-IIIa.[27] The distances used to construct the enzyme-bound arrangement, presented in Figure 5, allowed the phosphorus atom of the γ-phosphoryl group of ATP to be placed approximately 4 Å away from the oxygen atom of the 3′-OH group. Therefore, direct transfer of the phosphoryl group from ATP to amikacin may be the mechanism of phosphorylation. Also, the substrates are aligned so that only the 3′-oxygen is colinear with the P−O bond of the γ-phosphoryl group of ATP, which allows for the specific phosphorylation of the 3′-OH group in the presence of several other hydroxyl groups.

Butirosin A is 4,5-disubstituted at the 2-deoxystreptamine ring, and recent studies have shown that APH(3′)-IIIa-catalyzed phosphorylation can result in three different phosphorylation

(26) Mildvan, A. S.; Granot, J.; Smith, G. M.; Liebman, M. N. *Adv. Inorg. Biochem.* **1980**, *2*, 211.

(27) Thompson, P. R.; Hughes, D.; Wright, G. D. Manuscript in progress.

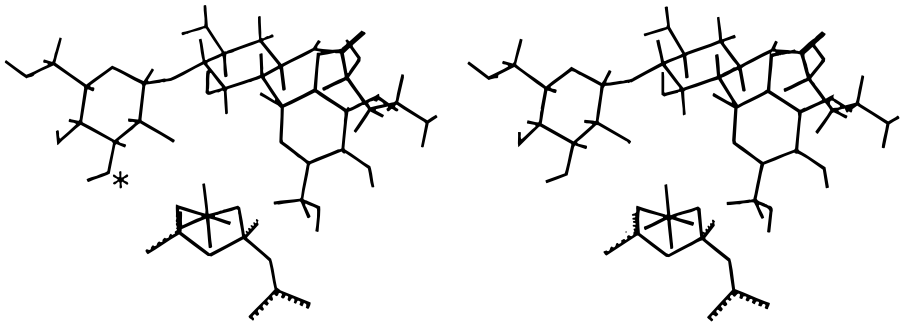

Figure 5. Proposed enzyme-bound arrangement of amikacin presented as a stereo pair. The distances that appear in Table 3 were used as constraints to construct these models, and all the Cr^{3+}-to-^1H distances in these models are within the error limits. Only the metal−triphosphate moiety of ATP is shown for clarity. The 3′-oxygen is denoted with an asterisk.

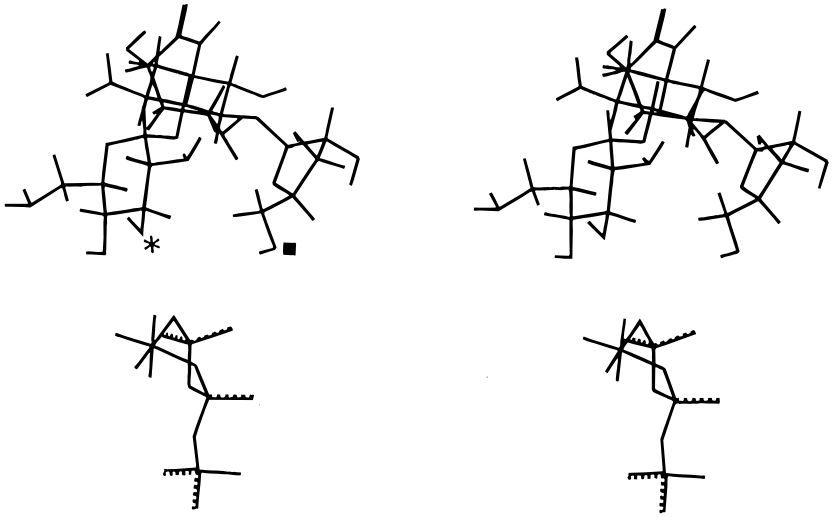

Figure 6. Proposed enzyme-bound arrangement of butirosin A presented as a stereo pair. The distances that appear in Table 3 were used as constraints to construct these models, and all the Cr^{3+}-to-^1H distances in these models are within the error limits. Only the metal−triphosphate moiety of ATP is shown for clarity. The 3′-oxygen is denoted with an asterisk, and the 5″-oxygen is denoted with a solid square.

products.[27] Butirosin A can be monophosphorylated at the 3′- or 5″-oxygen, or a diphosphorylated product can result in which both the 3′- and 5″-oxygens are phosphorylated. An arrangement was constructed (Figure 6) that satisfies the distance constraints and should also allow the different phosphorylation products to be produced. The distance constraints allow both the 3′-OH and 5″-OH to be placed into a position that is equidistant from the phosphorus atom of the γ-phosphoryl group. Even though neither of the two oxygen atoms in this arrangement is colinear with the P−O bond of the γ-phosphoryl group, it takes very little movement of the antibiotic to bring the 3′- or 5″-oxygen into a reactive position. An arrangement was also constructed in which the γ-phosphoryl group of ATP could be placed colinear with and 4 Å away from the 3′-OH. However, when CrATP was left in a fixed position and butirosin was rotated to bring the 5″-oxygen colinear with the P−O bond of the γ-phosphoryl group, the distance constraints could not be met. This suggests that butirosin may not have two productive modes of binding in which either the 3′-OH or 5″-OH can be brought into a reactive position with respect to ATP. Since butirosin A was found to be in fast exchange in the APH(3′)-IIIa·CrATP·butirosin ternary complex, it seems likely that the monophosphorylated butirosin product has to bind APH(3′)-IIIa again to be doubly phosphorylated. This implies that the active site of APH(3′)-IIIa is flexible such that a singly phosphorylated butirosin A product can still bind to the enzyme. This is also consistent with the kinetic mechanism which has recently been determined to be Theorell-Chance with ATP binding first followed by aminoglycoside, immediate release of phosphorylated antibiotic, and slow release of ADP.[28]

The conformation of butirosin A presented in Figure 6 has the 2,6-diamino-2,6-dideoxy-D-glucose and D-xylose rings in a stacking arrangement. The stacking arrangement of these rings was necessary to satisfy all distance constraints in any of the satisfactory enzyme-bound arrangements constructed for butirosin A. The above ring stacking was confirmed by transferred nuclear Overhauser effect (TRNOE) studies of butirosin A in the APH(3′)-IIIa·CaATP·butirosin ternary complex. A strong NOE cross-peak was observed between H-5″ and H-3′, as well as weaker NOEs between H-5″ and H-5′ and H-5″ and H-2′. These data indicate that the 2,6-diamino-2,6-dideoxy-D-glucose and D-xylose rings of butirosin A must be near each other. In addition to the above long-range NOEs, 13 additional NOEs were also observed which help to define the conformation of butirosin A around the two glycosidic linkages. The NOE constraints were used in energy minimization and dynamic routines (Sybyl, Tripos) that yielded a structure of butirosin A very similar to the one presented in Figure 6. In light of the above observations, one can strongly argue that the presence of other conformations/arrangements of butirosin A which satisfy the calculated Cr^{3+}-to-^1H distances and NOE data is highly unlikely. The enzyme-bound conformation of butirosin A described above is similar to the previously described solution structure of butirosin A.[23] Therefore, it seems that the enzyme

(28) McKay, G. A.; Wright, G. D. *J. Biol. Chem.* **1995**, *270*, 24686.

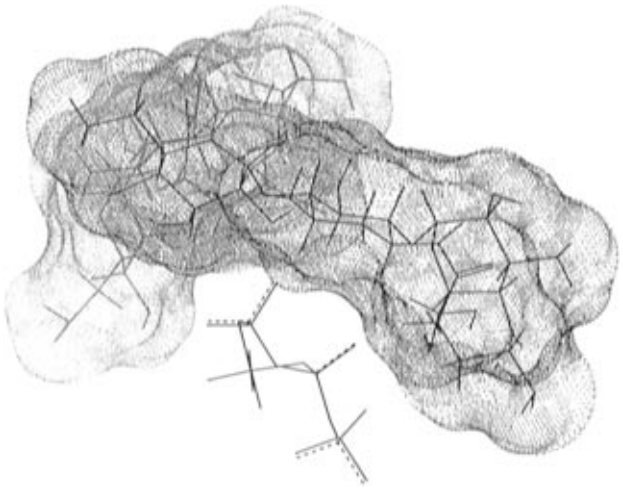

Figure 7. A superposition of the arrangements of amikacin (black) and butirosin A (gray) at the active site of APH(3′)-IIIa. The metal−triphosphate moieties presented in Figures 5 and 6 are superimposed, and the solvent surfaces were generated by rolling a H_2O molecule (1.4 Å diameter) over the surface of the antibiotics.

does not force butirosin A to adopt a conformation much different from that found in solution.

TRNOE studies of amikacin in the APH(3′)-IIIa·CaATP·-amikacin ternary complex also yielded results consistent with the arrangement and conformation of amikacin presented in Figure 5. This structure has the protons H-1′ and H-1″ within 4 Å of H-5 in the deoxystreptamine ring. Consistent with this structure, both of these expected NOE cross-peaks were observed in the TRNOE analysis. As expected, with the exception of NOEs across the glycosidic bonds, no other interring NOEs were observed. Thus, the conformations of both antibiotics shown in Figures 5 and 6 are supported by other NOE data.

Figure 7 has the metal−triphosphate complexes of Figures 5 and 6 superimposed and allows a direct comparison of the arrangement and conformation of enzyme-bound aminoglycosides. Figure 7 reveals that amikacin and butirosin A adopt different geometries at the active site of APH(3′)-IIIa. Amikacin has a more extended structure, due to its 4,6-disubstitution at the 2-deoxystreptamine ring, which allows Cr^{3+} and the triphosphate group of ATP to move in closer to the antibiotic. The compact shape of butirosin A prevents such an approach of the metal−nucleotide. This is reflected in the Cr^{3+}−proton distances presented in Table 3, where the distances in the amikacin ternary complex are significantly shorter. The compactness of butirosin A makes it more mobile at the active site and allows both the 3′- and 5″-OH groups to be extended out toward the γ-phosphoryl group at ATP. However, the extended structure of amikacin makes it more rigid at the active site and only allows the 3′-oxygen to be in a reactive position. Any movement of amikacin to bring another hydroxyl group into a reactive position (such as the 2′-OH) would be prevented by the triphosphate moiety of ATP.

The difference in binding of amikacin and butirosin A to the ATP·APH(3′)-IIIa binary complex observed here by NMR may hold the answer to a vexing problem. The K_m values for seven of eight aminoglycosides tested vary only by a maximum of 3.7-fold (9.3−34.3 μM) and all show substrate inhibition.[10] These include both 4,6- and 4,5-disubstituted aminocyclitol antibiotics. The lone aminoglycoside which does not fit this pattern is amikacin with a K_m 7−26-fold higher than the others and which does not show substrate inhibition. These differences may reflect a fundamental structural difference between the interactions of these aminoglycosides with APH(3′)-IIIa. The roughly perpendicular arrangement between the Cr−β,γ-phosphate complex observed here for butirosin A (Figure 7) may represent the preferred mode of binding of aminoglycosides to the enzyme. On the other hand, the extended conformation, roughly parallel to the Cr−β,γ-phosphate complex, exhibited by amikacin, does not result in efficient phosphorylation (due to either poor transfer in this conformation or difficulty obtaining a productive collision to form the ternary complex). The net result of this difference is that amikacin is poorly phosphorylated *in vivo* and is still a useful clinical drug, even in environments where APH(3′)s exist, while the other aminoglycosides are not.

Conclusion. The binding and relaxation data presented above show that amikacin and butirosin A adopt different arrangements and conformations at the active site of APH(3′)-IIIa. This is not unexpected because these antibiotics are substituted differently on the 2-deoxystreptamine ring. However, geometry information about these antibiotics is an important step in understanding how APH(3′)-IIIa modifies both 4,5- and 4,6-disubstituted aminoglycoside antibiotics and the regioselectivity unique to both types of antibiotics. This work is the first to describe the conformation and arrangement of aminoglycoside antibiotics bound to a modifying enzyme. In fact, the lack of structural information on this and other aminoglycoside phosphotransferase enzymes makes this study an important step in understanding the molecular mechanisms behind the inactivation of aminoglycoside antibiotics.

Recently, mechanism-based inactivators of 3′-phosphotransferases (types Ia and IIa) have been developed through modification of existing aminoglycoside antibiotics.[29] The current study is the first step in a program to design novel antibiotics and/or enzyme inhibitors based on the active site geometry of enzyme-bound antibiotics. This approach may lead to the discovery of compounds that can escape the many types of antibiotic inactivation employed by resistant strains of bacteria.

Acknowledgment. We would like to thank John Lamerdin and Dr. Baburaj Kunnummal from the Department of Biochemistry at The University of Tennessee for their help with the NMR spectroscopy. We would also like to thank Neil Whittemore and Ken Smith from the Department of Chemistry at The University of Tennessee for their help with the low-field NMR. The authors are grateful to Dr. David Baker for allowing us to use his Evans and Sutherland workstation and Sybyl modeling software. This work was supported by a grant from NIH (E.H.S.; GM-42661) and the Medical Research Council of Canada (G.D.W.).

JA952994C

(29) Roestamadji, J.; Grapsas, I.; Mobashery, S. *J. Am. Chem. Soc.* **1995**, *117*, 80.